Journal of Molecular Liquids 322 (2021) 114959

Contents lists available at ScienceDirect

Journal of Molecular Liquids

journal homepage: www.elsevier.com/locate/molliq

Enhanced electro-optic characteristics of polymer-dispersed nano-sized liquid crystal droplets utilizing PEDOT:PSS polymer composite

Srinivas Pagidi [a], Ramesh Manda [a], Hoon Sub Shin [a,b], Junhyeok Lee [a], Young Jin Lim [a], MinSu Kim [c,*], Seung Hee Lee [a,*]

[a] Department of Nanoconvergence Engineering and Department of Polymer-Nano Science and Technology, Jeonbuk National University, Jeonju, Jeonbuk 561-756, Republic of Korea
[b] LG Display Co., Ltd., Gumi, Gyungbuk, South Korea
[c] Department of Physics and Astronomy, Johns Hopkins University, Baltimore, MD 21218, USA

ARTICLE INFO

Article history:
Received 25 August 2020
Received in revised form 11 November 2020
Accepted 3 December 2020
Available online 06 December 2020

Keywords:
Electro-optic materials
Liquid crystals
PEDOT:PSS
Dielectric permittivity
Kerr constant

ABSTRACT

Flexible devices require much higher reliability upon device driving. Because the *voltage-driven* liquid crystal devices show higher reliability than *current-driven* devices, flexible liquid crystal devices are relatively suit to open a new application fused with flexible electronics in displays and photonic devices. One plausible approach is to utilize polymer-dispersed liquid crystals with nanoscale droplets of liquid crystals dispersed in a polymer matrix. One of the most significant shortcomings with that approach is high operating voltage due to the strong molecular interaction between liquid crystals and polymer matrices, low fill factor of the system, and a voltage drop in the dielectric polymer matrix. Herein, we show a polymer composite that is blended with conductive PEDOT:PSS polymer to enhance the dielectric property of the system. The composite polymer matrix we show in this work provides a pathway of electric fields via the PEDOT:PSS when applying voltages and eventually reduces the voltage drop in the composite matrix. As a consequence of the enhanced electric field, the Kerr constant and transmittance of probe light passing through the sample mixing with 3.5 wt% of PEDOT:PSS increases up to 11.7 and 37.3% and the operating field decreases up to 17.2%. Furthermore, the rising times are enhanced up to 30% while the decaying times remain the same. We believe that this approach will greatly contribute to the realization of flexible liquid crystal devices.

1. Introduction

In the past few decades, liquid crystals (LCs) have been one of the most remarkable materials used in the field of flat panel displays owing to their unique properties including dielectric and optical anisotropies. In the future, devices that play a role in mediating communications at the human/machine interface are required to be flexible to meet all requirements of flexible electronics. Despite the successful industrial history, unfortunately, LCs are disadvantageous on flexible substrates because the anisotropy is highly dependent on the optical and electrical vectorial directions. Organic light-emitting devices are known as being ideal for flexible displays, but liquid crystal displays (LCDs) are still advantageous from perspectives of strong reliability, the fabrication process, yield point, and cost. Several methods have been proposed to make flexible LCDs work such as fabrication of polymer walls/fibers and the use of polymer substrate [1–5]. These methods show good bendability, but the uniformity of LC orientation is easily broken and field-response is distorted upon bending [5]. Unlike the polymer walls, polymer-dispersed liquid crystals (PDLCs) with nano-sized LC droplets in the polymer matrix (nano-PDLC) is a flexible polymer film itself. Consequently, perturbation of the LC orientation occurs relatively less upon bending stress compared to the polymer wall approach, i.e., its electro-optic characteristics are well preserved under bending stress so that its applicability to flexible substrates is better.

In nano-PDLC with the size of LC droplets <300 nm, interference between the LC droplets and visible light is too small to have light scattering and it guarantees the optically isotropic liquid crystal (OILC) system. Utilization of the OILC system for display devices has several advantages such as fast switching time, high-contrast ratio, and wide and symmetric viewing angle without optical compensation films [6–10]. Furthermore, the electro-optic performances like transmittance, switching time and the contrast ratio are preserved upon mechanical bending of the optical films [7,11–13]. Despite numerous merits, typical concentration of monomers requires >50% to achieve efficient optical isotropy in the nano-PDLC system [12–15]. Such large amount of polymer affects low Kerr (K) constant of the nano-PDLC system ($K \sim 0.75$ nm/V^2) because such system has low filling factor and limited physical properties: birefringence (Δn) and dielectric anisotropy ($\Delta\varepsilon$) [16,17]. Herein, K is related to $\Delta n \Delta\varepsilon R^2/K_{LC}\lambda$, where R is the radius of LC droplets and K_{LC} is

* Corresponding authors.
E-mail addresses: mkim182@jhu.edu (M. Kim), lsh1@chonbuk.ac.kr (S.H. Lee).

https://doi.org/10.1016/j.molliq.2020.114959
0167-7322/

the elastic constant of LCs with one-constant approximation, indicating that the parameters Δn, $\Delta\varepsilon$, R should be large enough for achieving maximum K of the system [17]. However, increase in length scale of either R or Δn of LCs causes light scattering. On the other hand, increase in $\Delta\varepsilon$ of LCs can cause increase in viscosity of the LCs, resulting in relatively slow response time. Using a LC with high Δn and $\Delta\varepsilon$, high $K \sim 13.7$ nm/V^2 was reported in polymer-stabilized blue phase LC but it has another issue like phase instability during electro-optic switching [18], unless the well-treated surface condition is not met [19]. In summary, to lower operating voltage, increase in the magnitude of K by optimizing only physical properties of LC will result in some loss of its electro-optic performances such as high contrast ratio and fast response time.

A few reports on improving electro-optics of nano-PDLC show that doping a small amount of functionalized-carbon nanotubes (f-CNTs) [20], reduces an operating voltage and using chiral molecules [21] or acrylate monomer mixtures [22,23], reduces light scattering in a field-off state. The weakest point among all aspects of the nano-PDLC for application to display devices is high operating voltage. As a solution, we pay attention to a method to enhance the conductivity of the polymer matrix. In this approach, we can avoid the abovementioned electro-optic performance drop by enhancing the $\Delta\varepsilon$ and Δn of LCs. Although we find that mixing of nano-PDLC with f-CNTs is favorable especially for minimizing the field-screening effect inside the polymer matrix [20], the miscibility issue still remains when mixing with the LC/monomer mixture because it limits doping concentration of f-CNTs in a composite blend. From this perspective, we believe that the incorporation of conductive polymer inside the insulating polymer is favored because good miscibility in polymer to polymer mixture is expected in general. One good candidate is a widespread-used high conductive and transparent polymer, poly(3,4-ethylene dioxythiophene):poly(styrene sulfonate) (PEDOT:PSS) [24,25].

In this work, thus, we utilize conductive PEDOT:PSS polymer, doping it with a reference nano-PDLC mixture. Again, we expect the miscibility is much higher than that with f-CNTs so that the conductivity of the composite matrix can be adjusted far higher. As a consequence of this approach, the conductivity of the polymer matrix can be significantly enhanced and it conveys to minimize the voltage drop along the polymer matrix. We investigate how the dielectric property of the nano-PDLC system contributes to the electro-optic properties such as field-dependent transmittance, the Kerr constant, and switching response times.

2. Switching principle of the proposed device

Schematic cell structure and orientation of nano-sized LC droplets embedded in a polymer matrix doped with conductive polymer PEDOT:PSS is shown in Fig. 1. The doped conductive polymer is monodispersed in the host polymer matrix so that the additives are guaranteed to influence on the entire system. In the field-off state, the LC droplets with bipolar LC configuration inside the droplets in general and their sizes below visible wavelength are randomly oriented, rendering the nano-PDLC system optically isotropic. In the field-on state, the field generated between electrodes reorients the optic axis of LC along the field direction, giving rise to phase retardation. Under crossed polarizer, its transmittance behavior follows as [26],

$$\frac{T}{T_0} = \sin^2 2\psi \sin^2\left(\frac{\pi d\Delta n_{ind}}{\lambda}\right), \tag{1}$$

where ψ is the angle between the optic axis of field-induced LC and the transmittance axis of the polarizer, d is the effective thickness of the induced birefringence layer and Δn_{ind} is the effective induced birefringence of LC layer in which both values are spatially modulated due to the interdigitated electrodes. In the field-off state, the device exhibits a dark state since Δn_{ind} is zero, and in the field-on state with conditions of $\psi = \pi/4$ and $d\Delta n_{\mathrm{ind}} = \lambda/2$, the device exhibits a maximal transmittance.

In the nano-PDLC system, the Δn_{ind} is associated with K as follows $\Delta n_{\mathrm{ind}} = \lambda K E^2$ where E is applied field strength [27]. The threshold field (E_{th}) of the device changes with respect to the concentration of PEDOT:PSS in the polymer composite matrix since the conductivity of the polymer matrix depends on the doping concentration ϕ. Under such assumption of the conductive medium in the host polymer matrix, the E_{th} can be determined as [20,28],

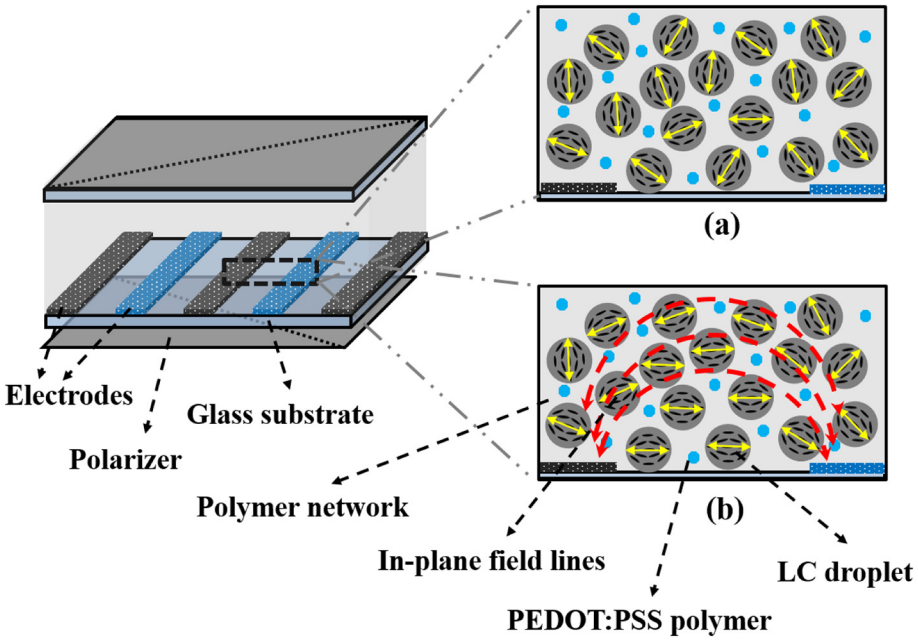

Fig. 1. Schematic representation of the conductive-polymer PEDOT:PSS-doped nano-PDLC system driven by interdigitated electrodes: (a) Randomly oriented LC droplets with size less than the wavelength of visible light at field-off state and (b) Orientation of optic axis along the field directions in the field-on states.

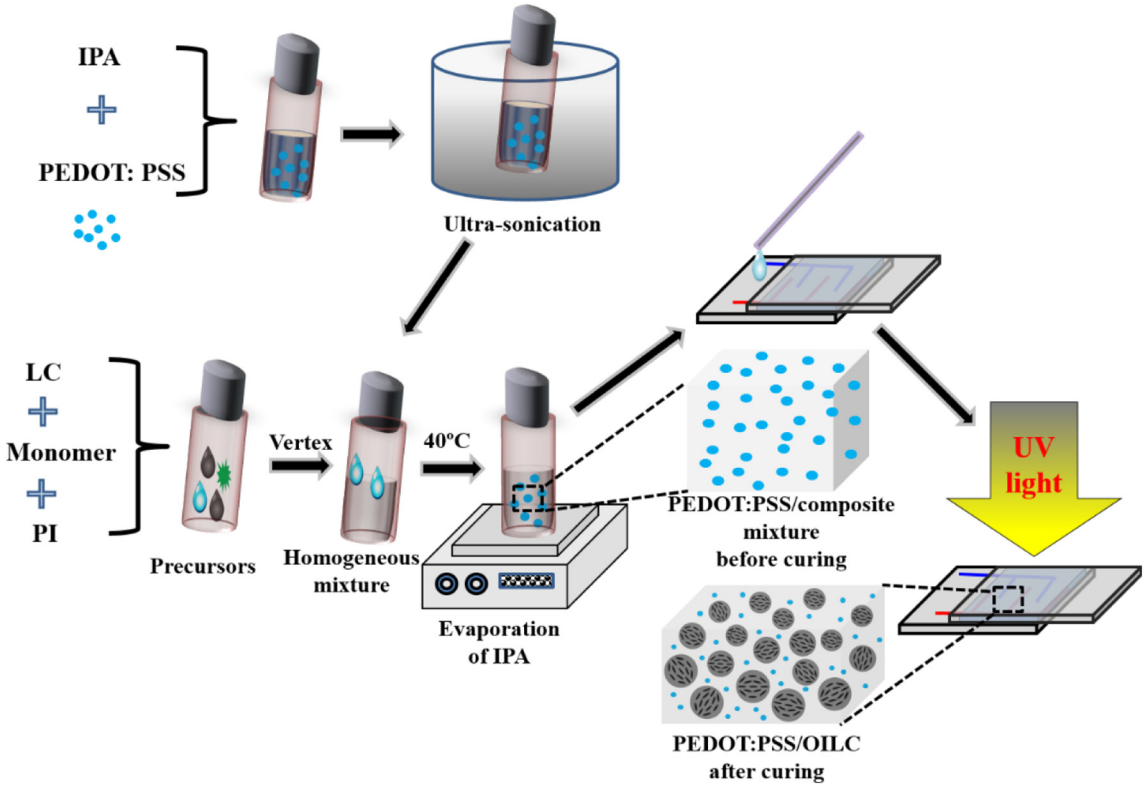

Fig. 2. Experimental procedure of PEDOT:PSS doped nano-PDLC sample.

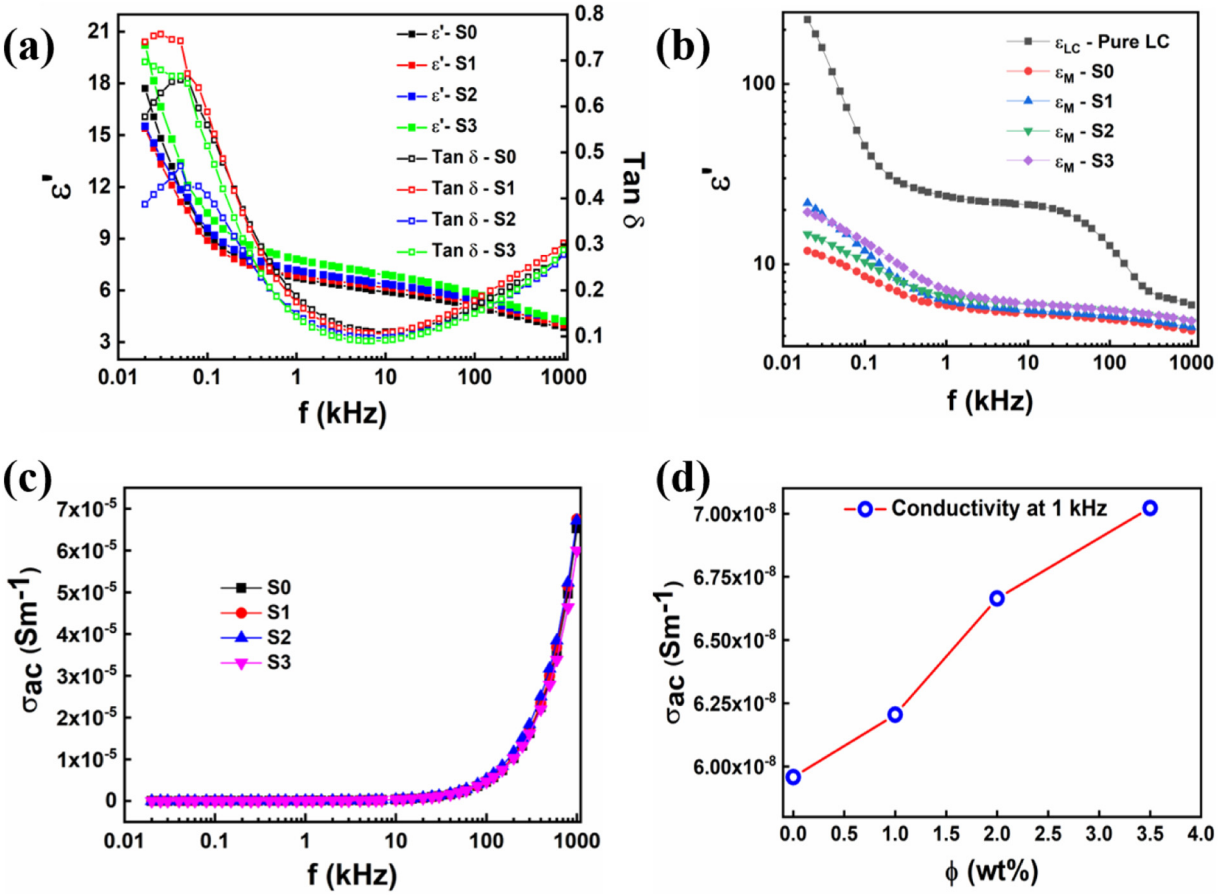

Fig. 3. The dielectric properties of the PEDOT:PSS-doped LC/polymer composites measured as a function of frequency *f*. (a) The real part of relative permittivity ε' and loss tangent $tan\delta = \varepsilon''/\varepsilon'$, (b) The measured ε' of pure LC (ε_{LC}) and LC removed polymer cells (ε_M). (c) Conductivity σ_{ac}. (d) The estimated conductivity σ_{ac} as a function of dopant concentration ϕ at $f = 1$ kHz.

$$E_{th} \approx \frac{1}{c}\frac{\pi}{R}\sqrt{\frac{K_{LC}}{\varepsilon_0 \Delta\varepsilon}}, \tag{2}$$

where c is the pre-factor that is expressed as,

$$c \approx \frac{3\varepsilon_M}{\varepsilon_{LC} + 2\varepsilon_M}, \tag{3}$$

where ε_M is the effective dielectric constant of the polymer matrix and ε_{LC} is the dielectric constant of the host LC. Therefore, the pre-factor c should be larger than 1 in order to reduce E_{th} while the droplet size and physical properties of LC remain unchanged. The doping of conductive medium inside the polymer matrix increases the magnitude of c, resulting in increased conductivity of the polymer matrix. Owing to this effect, the voltage drop in the insulating polymer matrix can be minimized giving rise to the field enhancement effect. Consequent to this, the applied field strength to reorient LCs inside the nano-sized LC droplets is reduced and the effect becomes more pronounced with increasing the dopant concentration ϕ, thus leading to reduction of the E_{th}. Electro-optic response times of rise (τ_{on}) and decay (τ_{off}) in nano-PDLC are defined as follows [29,30],

$$\tau_{on} \approx \frac{\gamma}{\frac{\Delta\varepsilon\varepsilon_0 c^2 E^2}{4\pi} - \frac{K_{LC}}{R^2}}, \tag{4}$$

$$\tau_{off} \approx \frac{\gamma R^2}{K_{LC}}, \tag{5}$$

where γ and K_{LC} are rotational viscosity and elastic constant of LC, respectively and R is the size of LC droplets in a polymer matrix. From Eq. (4), one can understand that increasing the field strength gives rise to faster τ_{on} if other physical parameters remain the same. Consequently, we expect the doping of the conductive polymer induces faster τ_{on}.

3. Experimental procedure

3.1. LC/polymer mixtures

We used a LC, MLC-2053 ($\Delta\varepsilon = 42.6$ at 1 kHz, $T_{NI} = 86$ °C, Merck Advanced Technology, Korea); host monomers, PN393 ($n_p = 1.473$ at 589 nm) and TMPTA (Trimethylolpropane Triacrylate) ($n_p = 1.474$ at 589 nm); a photo-initiator (PI), Irgacure-651 (Irg-651); and a high-conductive polymer (PEDOT:PSS, Sigma Aldrich). The reference nano-PDLC mixture consists of LC / PN393 / TMPTA / Irg-651 (42 / 47.75 / 10 / 0.25) and three-sample mixtures are prepared as the reference mixture is mixed with the dopant polymer PEDOT:PSS by the concentration $\phi = 1$, 2 and 3.5 wt%, naming the samples S0, S1, S2, and S3, respectively.

3.2. Cell preparation

The PEDOT:PSS was at first uniformly dissolved into isopropyl alcohol (IPA) and then it was mixed with LC/monomer mixture. Then, the total mixture was ultrasonicated for 2 h at elevated temperatures to improve the dispersion of the dopant polymer. After that, the IPA was evaporated by placing the sample mixtures over a hot plate while stirring it at 80 °C. The resultant mixture was capillary-injected into test cells at 90 °C, with a one-plain glass substrate and the other interdigitated indium tin oxide (ITO) electrode substrate, where the electrode width (w) and spacing (l) between them are 4 μm. The cell thickness is 10 μm for all cells. Once the mixture was fully loaded into the cell, and UV light at 110 mW/cm^2 was exposed for 6 mins. The detailed

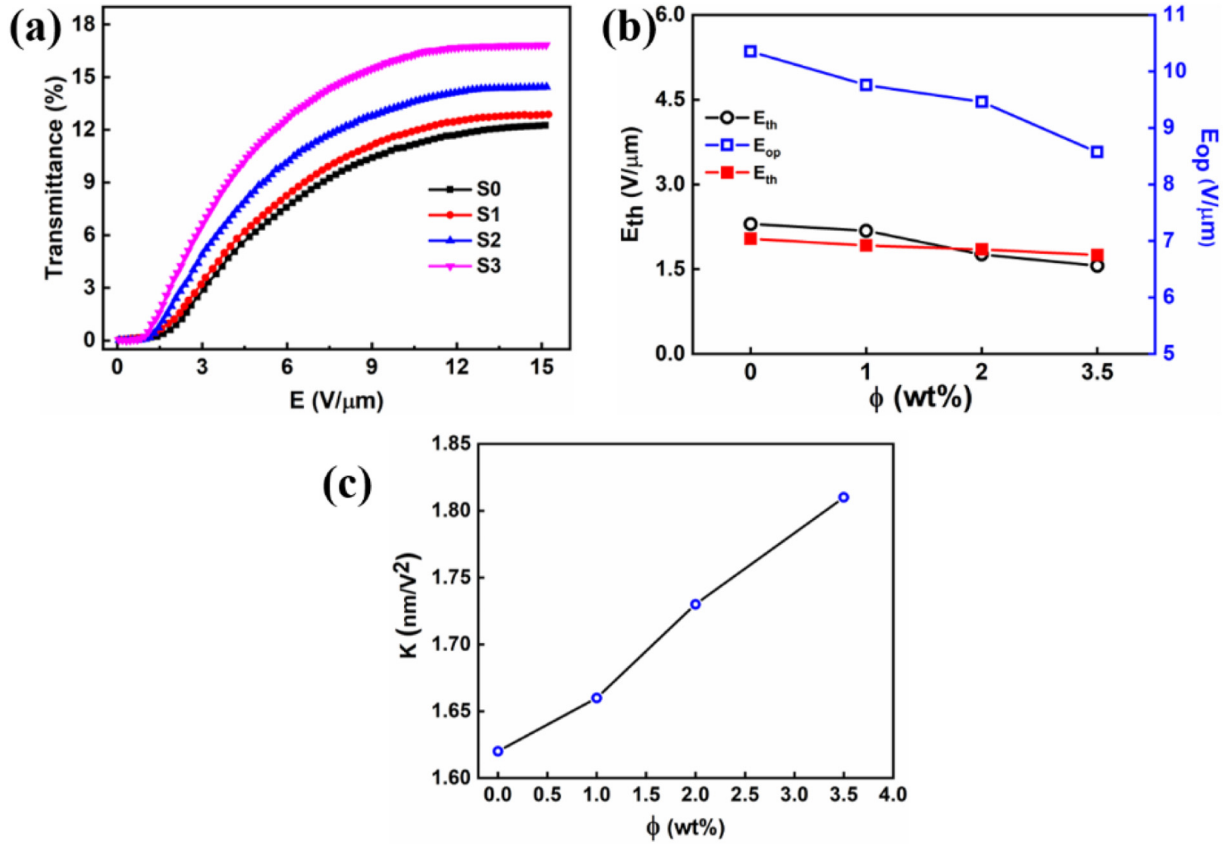

Fig. 4. The electro-optic properties of the PEDOT:PSS-doped LC/polymer composites. (a) Electric field-dependent transmittance curves, (b) Measured threshold E_{th} (the calculated E_{th} is in red color) and operating E_{op} and (c) Measured Kerr constant K as a function of ϕ.

schematic diagram for the preparation of PEDOT:PSS doped nano-PDLC composite is clearly shown in Fig. 2.

3.3. Characterization

The test cells were examined by a polarizing optical microscope (POM) (ECLIPSE E600, Nikon, Japan) and the field off/on state images are captured using an equipped CCD (DXM 1200, Nikon). We used commercial software (*i*MT *i*-Solution Inc., Canada) for measuring the light leakages of the POM images captured in the field-off state. The electro-optic properties were evaluated by using a setup consisting of a photodetector (DET36A/M, 350–1100 nm, Thorlabs), a function generator (33521A, Agilent) and an oscilloscope (DPO 2024B, Tektronix). The E_{th} and E_{op} are determined as the field to reach 10% and 90% of maximal transmittance, respectively. The resultant mixtures were phase-separated between ITO electrodes and then we used a precision LCR meter (4284A, Agilent) with the frequency range of 20 Hz $< f <$ 1000 kHz for determining the frequency dependence of the complex dielectric function relation defined as the $\varepsilon^*(f) = \varepsilon'(f) - i\varepsilon''(f)$, where ε' and ε'' are the real and imaginary part of the dielectric permittivity. The ε' of the test cells were calculated using the relation, $\varepsilon' = C_p/C_0$, where C_p is the relative capacitance of the test cells that are infiltrated with the sample mixtures and C_0 is the capacitance of empty cell, $C_0 = \varepsilon_0 A/d$, where A and d are the related electrode area and the cell thickness, respectively. The LC was washed away by soaking test cells in the *n*-hexane for 24 h to measure the dielectric properties of polymer matrices ε_M without LC, whereas the conventional procedure was used for measuring the ε_{LC} of pure LC using the same d. Furthermore, we also calculated the loss tangent $tan\delta = \varepsilon''/\varepsilon'$ [31]. The LC removed test cells were separated using the sharp-edged blade to get a polymer matrix and then a conductive gold layer was coated using radio frequency (RF) sputtering in order to avoid charge accumulation over the insulating polymer matrix. The substrates were used to observe the morphology of the polymer network by a field emission scanning electron microscope (FESEM).

4. Results and discussion

In this section, we aim to investigate the electro-optic properties associated with the effects of doping PEDOT:PSS into a nano-PDLC composite. We organize our results of electro-optic characterization into three subsections. In the first subsection, we measure the relative permittivity and conductivity properties. In the second subsection, the electric field-dependent transmittance and response times upon field on/off states are measured. In the third subsection, lastly, the POM images and surface morphology of the polymer matrix are investigated.

4.1. Dielectric properties

Frequency-dependent relative permittivity ε' and loss tangent $tan\delta$ to verify the dielectric properties are measured as shown in Fig. 3a. As increasing the frequency, the ε' of all samples decreases and the measured $tan\delta$ shows typical curves of the imaginary part that is related to the real part. As the PEDOT:PSS concentration ϕ changes, at 1 kHz, ε' is measured to be 6.72, 6.85, 7.16 and 7.80 for the samples S0, S1, S2, and S3, respectively. The ε' of the sample S1, S2, S3 increases by about 2, 6.5, 16.2%, respectively, compared to the sample S0.

In order to estimate the pre-factor c in Eq. (2), we measure the ε_{LC} and ε_M as shown in Fig. 3b. At $\phi = 1$ kHz, we measure the relative permittivity of pure LC cell and polymer network (LC-removed) cells, $\varepsilon_{LC} =$ 23.83 and $\varepsilon_M = 5.90, 6.26, 6.63, 7.20$ for S0, S1, S2, S3, respectively. Then, the c is calculated as 0.49, 0.52, 0.54, 0.57. As the PEDOT:PSS concentration in the polymer ϕ increases in the samples, the c increases.

The frequency-dependent conductivity is measured as shown in Fig. 3c. It shows the σ_{ac} increases as increasing the dopant concentration ϕ as well as f. In order to quantify the AC conductivity of the test samples, we calculate it based on the formula $\sigma_{ac} = 2\pi f\varepsilon_0\varepsilon' tan\delta$ [31]. The calculated σ_{ac} is 5.68×10^{-8}, 6.20×10^{-8}, 6.66×10^{-8} and 7.10×10^{-8} S/m, respectively, for the samples S0, S1, S2, and S3 at $f = 1$ kHz as shown in Fig. 3d. As compared to S0, the σ_{ac} of the samples is increased by 9.15%, 17.25%, and 25% for samples S1, S2, and S3, respectively.

The dielectric property and conductivity are enhanced as ϕ increases. This implies that the uniform distribution of the conductive polymer in the host insulating polymer matrix helps the immobile charges to be better polarized. We believe the conductive polymer dopant in the composite film not only provides electrons to flow easier in the polymer matrix but also suppresses the dissipation of the given electric energy upon the electrical polarization in the material.

4.2. Field-dependent transmittance curves and response times

Fig. 4a shows the electric field-dependent transmittance curves of the samples S0, S1, S2, and S3. In the field-off state, the transmittance of the samples is 0.047, 0.050, 0.052, and 0.051, respectively, which indicate similar dark levels regardless of the conductive dopant concentration ϕ. As the electric field strength ramps up, the transmittance increases up to peak points of each curve. At the peaks, where the degree of the LC reorientation in the droplets becomes maximum, $T_{S0} < T_{S1} < T_{S2} < T_{S3}$. The field-on maximum transmittance of the S1,

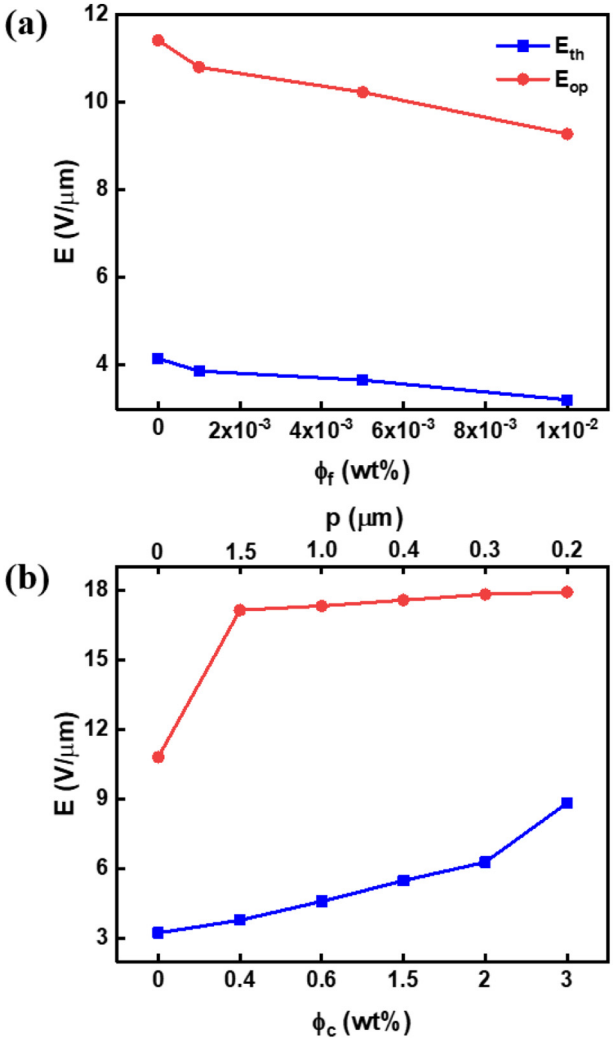

Fig. 5. Measured E_{th} and E_{op} as a function of (a) f-CNTs concentration ϕ_f and (b) a chiral dopant (SRM17) concentration ϕ_c and chiral pitch p.

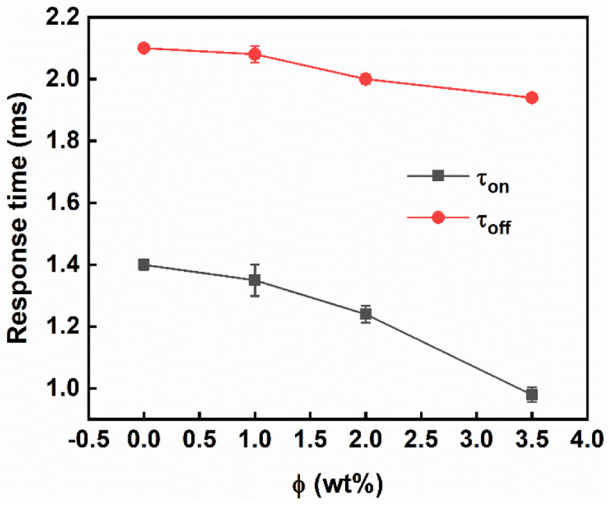

Fig. 6. The measured and estimated electro-optic response times of PEDOT:PSS-doped LC/polymer composites.

S2, and S3 is enhanced by ~5.06, ~17.87, and ~37.30% as f increases in comparison to that of the reference sample. As the pre-factor c increases, E_{th} decreases. At $E > E_{th}$, the field-induced refractive index Δn_{ind} (E) becomes higher. Then, the transmittance should get higher at the same E.

The measured E_{th} and E_{op} of the S0, S1, S2, S3 are 2.30, 2.18, 1.76, 1.56 and 10.35, 9.76, 9.46, 8.57, respectively, as shown in Fig. 4b, indicating the E_{th} and E_{op} of the S1, S2, S3 are reduced from S0 by about 6.5, 22.6, 32.2% and 5.7, 8.6, 17.2%, respectively. The E_{th} is also theoretically estimated from Eq. (2) with the estimated pre-factor c of each sample and it shows good agreement with experimental data, as shown in Fig. 4b, proving doping the conductive dopant can decrease operating voltage. Nevertheless, increasing ϕ up to 4 wt% the cell does not show much improvement in the E_{th} and E_{op} compared to S3 and the resultant mixture exhibits little bluish color in appearance, decreasing the transmittance.

The Kerr constant which determines operating voltage is estimated based on the variation of field-induced birefringence Δn_{ind} as a function of electric field E^2 as shown in Fig. 4c. The magnitude of K for the sample S1 to S3 is increased by 2.5, 6.8, and 11.7% compared to that of the reference sample S0. This explains the reduced E_{th} and E_{op} in all conductive polymer doped cells.

To verify the improvement with respect to the previously reported results, we compare the measured E_{th} and E_{op} of conductive PEDOT:PSS doped nano-PDLCs to f-CNTs [20] and a chiral dopant (SRM17) [21] doped ones. As shown in Fig. 5a and b, when doping f-CNTs and varying the concentration of f-CNTs as 1×10^{-3}, 5×10^{-3}, 1×10^{-2}, E_{th} decreases by 6.8, 11.74, 22.5% and E_{op} decreases by 5.36, 10.36, 18.71%, respectively. Doping f-CNTs contributes to similar aspect in terms of the applying electric field as what PEDOT:PSS does. However, the doping rate is quite different: f-CNTs aggregate themselves even with much smaller doping concentration because of the strong van der Waals interactions, which, in turn, in case the dispersion can be well controlled for both dopants, f-CNT would possess much larger potential to contribute to the electro-optic performance. On the other hand, doping a chiral dopant (SRM17) results in the other tendency that the E_{th} and E_{op} increase as more the chiral dopant we add. The twist in the molecular arrangement requires more dielectric energy for unwinding it.

The smaller the size of LC droplets R in the polymer matrix, the faster the response times, which can be explained by Eqs. (4), (5). We apply 15 V/mm at 1 kHz to measure the τ_{on} and τ_{off} times, that is defined as the time taken for the transmittance change from 10% and 90% in the field-on state and 90% and 10% in the field-off state, respectively. The measured τ_{on} is 1.40, 1.35, 1.24, and 0.98 ms and τ_{off} is 2.10, 2.08, 2.00 and 1.94 ms for the sample S0, S1, S2, and S3, respectively, as shown in Fig. 6. It is noticeable that as c increases, the τ_{on} becomes faster by 3.5, 11.4 and 30.0%, for the sample S1, S2, and S3, respectively, compared to the sample S0 while τ_{off} remains almost the same. Faster rise response time with the same applied fields could be possible evidence for increased applied field strength to nano-sized LC droplets inside the polymer matrix.

4.3. Polarizing optical microscopy

Fig. 7 shows POM images of the samples S0, S1, S2, and S3. In the absence of field, the cells show a good dark state with about the same level and the dark state remains invariant upon rotation of the samples in-plane under crossed polarizers, indicating all the sample cells are optically isotropic. From the obtained similar dark levels of the POM images, we can anticipate two points: 1) the dark state is independent on the doping concentration ϕ; 2) the system is in the Rayleigh-Gans

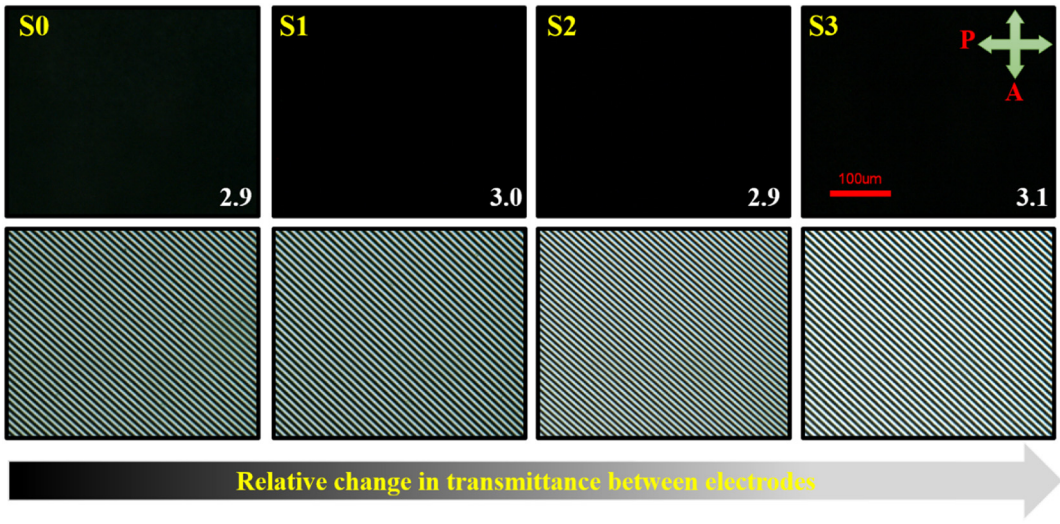

Fig. 7. POM images of four different cells under crossed polarizers when an applied electric field is off (top row) and on with $E = 15$ V/μm (bottom row). The numbers in a dark state as an inset indicate the relative brightness of the images (top row). P and A represent polarizer and analyzer.

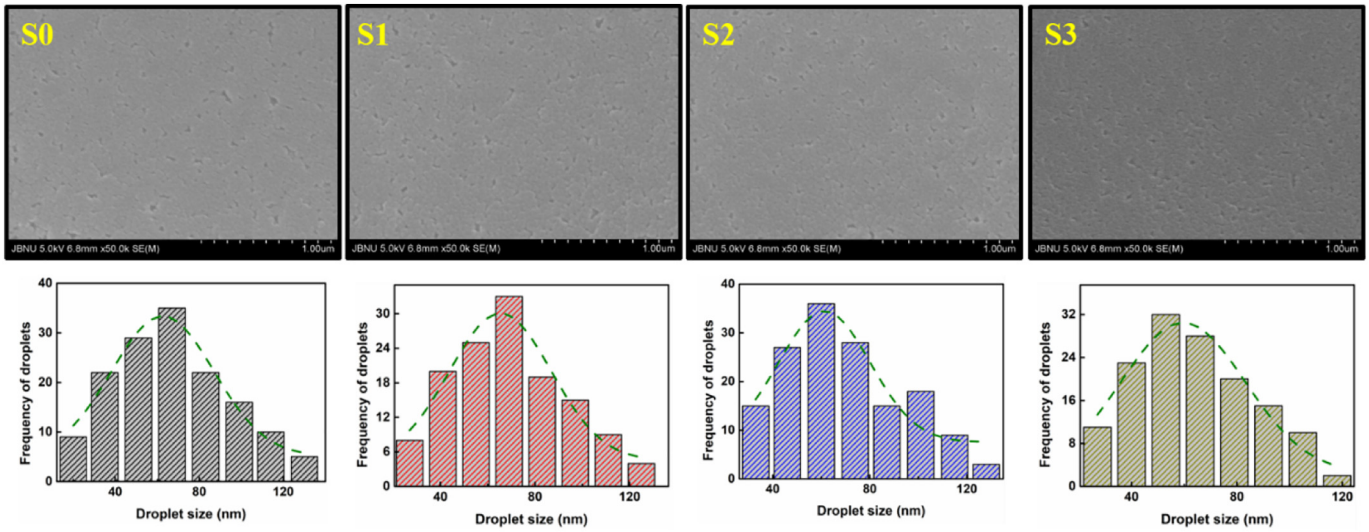

Fig. 8. FESEM images of polymer morphologies (top row) and related droplet size distribution with Gaussian fits (bottom row).

Table 1
Electro-optic properties of the samples.

Sample	ϕ [a] [%]	c [b]	R [c] [nm]	ε' [d]	$tan\ \delta$ [e]	σ_{ac} [f] [S/m]	E_{th} [g] [V/μm]	E_{op} [h] [V/μm]	K [i] (nm/V^2)	τ_{on} [j] [ms]	τ_{off} [k] [ms]
S0	0	0.49	62.60 ± 2.07	6.72	0.187	5.68×10^{-8}	2.30	10.35	1.62	1.40	2.10
S1	1	0.52	65.34 ± 2.45	6.85	0.174	6.20×10^{-8}	2.18	9.76	1.66	1.35	2.08
S2	2	0.54	61.30 ± 3.10	7.16	0.149	6.66×10^{-8}	1.76	9.46	1.73	1.24	2.00
S3	3.5	0.57	59.60 ± 2.11	7.80	0.143	7.10×10^{-8}	1.56	8.57	1.81	0.98	1.94

[a] PEDOT:PSS concentration; [b] The pre-factor in Eq. (2); [c] The size of LC droplets; [d,e] The relative permittivity and loss tangent; [f] AC conductivity; [g,h] Threshold and operating electric field strengths; [i] Kerr constant; [j,k] Rise and decay response times. All measurements were performed at $f = 1$ kHz.

approximation regime that explains the relation between the average scattering cross-section a_s and the wavelength of light l or the size of LC droplets R, that is, $\alpha_s \propto \lambda^{-4}R^6$ [32]. Upon applying field, the birefringence is induced and bright regions between electrodes appear. We note that the brightness of the POM images is enhanced as f increases, which is in good agreement with the result shown in Fig. 4a.

4.4. Polymer morphology

To verify the droplet size, we observe the polymer networks using FESEM after washing away the LCs from the polymer matrix. Fig. 8 shows the surface morphology of the polymer networks and droplet size distributions. The mean droplet size is measured as $R = 62.60 \pm 2.07$, 65.34 ± 2.45, 61.30 ± 3.10, and 59.60 ± 2.11 nm for the samples of S0, S1, S2, and S3, respectively. The droplet size is more or less consistent over the samples and the morphology shows no specific aggregation of the conductive polymer dopants. The irregular shape of the droplet formation comes from a fast curing rate of the acrylate-based monomers. With the droplet size less than 100 nm, the samples are transparent with no severe scattering.

5. Conclusion

We have fabricated an optically isotropic nano-PDLC unit cell whose droplet size is subwavelength of visible light and whose host polymer matrix is doped with PEDOT:PSS conductive polymer for electro-optic property enhancement. The concentration of PEDOT:PSS influences the electro-optic properties in the LC/polymer composite. As the concentration of PEDOT:PSS increases, the relative permittivity is enhanced and thus the pre-factor c in Eq. (3) becomes improved. This improvement gives rise to enhancement of overall transmittance, threshold, operating voltage, and response times.

The PEDOT:PSS polymer provides electrons a pathway to more freely flow in the polymer matrix and suppress the dissipation of the given electric energy upon the electrical polarization in the material. The results show improved dielectric permittivity, conductivity, brightness (transmittance), and electro-optic properties, including response times upon electric field application as details remarked in Table 1. We believe the result would effectively contribute to improve the electro-optic properties and provide a good approach to resolve remaining issues towards the realization of flexible devices.

Declaration of Competing Interest

There are no conflicts to declare.

Acknowledgments

This research was supported by the Basic Science Research Program through the National Research Foundation of Korea (NRF) funded by the Ministry of Education (2016R1D1A1B01007189) and by the National Research Foundation of Korea (NRF) grant funded the Korea government (MSIT) (No. 2019R1A5A8080326).

References

[1] Y. Kim, J. Francl, B. Taheri, J.L. West, A method for the formation of polymer walls in liquid crystal/polymer mixtures, Appl. Phys. Lett. 72 (18) (1998) 2253–2255.
[2] H. Fujikake, T. Aida, J. Yonai, H. Kikuchi, M. Kawakita, K. Takizawa, Rigid formation of aligned polymer fiber network in ferroelectric liquid crystal, Jpn. J. Appl. Phys. 38 (9R) (1999) 5212.

[3] J.-W. Jung, S.-K. Park, S.-B. Kwon, J.-H. Kim, Pixel-isolated liquid crystal mode for flexible display applications, Jpn. J. Appl. Phys. 43 (7R) (2004) 4269.
[4] T. Ishinabe, H. Sakai, H. Fujikake, 37.4 L: Late-News Paper: High Contrast Flexible Blue Phase LCD with Polymer Walls, SID Symposium Digest of Technical Papers, Wiley Online Library, 2015 553–556.
[5] Y.T. Kim, J.H. Hong, S.D. Lee, Fabrication of a highly bendable LCD with an elastomer substrate by using a replica-molding method, J. Soc. Inf. Disp. 14 (12) (2006) 1091–1095.
[6] S. Matsumoto, M. Houlbert, T. Hayashi, K.I. Kubodera, Fine droplets of liquid crystals in a transparent polymer and their response to an electric field, Appl. Phys. Lett. 69 (8) (1996) 1044–1046.
[7] S. Matsumoto, Y. Sugiyama, S. Sakata, T. Hayashi, Electro-optic effect, propagation loss, and switching speed in polymers containing nano-sized droplets of liquid crystal, Liq. Cryst. 27 (5) (2000) 649–655.
[8] M.S. Kim, L.-C. Chien, Topology-mediated electro-optical behaviour of a wide-temperature liquid crystalline amorphous blue phase, Soft Matter 11 (40) (2015) 8013–8018.
[9] M.S. Kim, Liquid Crystalline Amorphous Blue Phase: Tangled Topological Defects, Polymer-Stabilization, and Device Application, Kent State University, 2015.
[10] M.S. Kim, Y.J. Lim, S. Yoon, M.-K. Kim, P. Kumar, S.-W. Kang, W.-S. Kang, G.-D. Lee, S. Hee Lee, Luminance-controlled viewing angle-switchable liquid crystal display using optically isotropic liquid crystal layer, Liq. Cryst. 38 (3) (2011) 371–376.
[11] Y. Tanabe, H. Furue, J. Hatano, Optically isotropic liquid crystals with microsized domains, Mater. Sci. Eng. B 120 (1–3) (2005) 41–44.
[12] R. Manda, S. Pagidi, Y.J. Lim, R. He, S.M. Song, J.H. Lee, G.-D. Lee, S.H. Lee, Self-supported liquid crystal film for flexible display and photonic applications, J. Mol. Liq. 291 (2019) 111314.
[13] R. Manda, J.H. Yoon, S. Pagidi, S.S. Bhattacharyya, D.T.T. Tran, Y.J. Lim, J.-M. Myoung, S.H. Lee, Like flexible optically isotropic liquid crystal film for tunable diffractive devices, Opt. Express 27 (24) (2019) 34876–34887.
[14] J.L. West, Phase separation of liquid crystals in polymers, Molecular Crystals and Liquid Crystals Incorporating Nonlinear Optics 157 (1) (1988) 427–441.
[15] S. Pagidi, R. Manda, S.S. Bhattacharyya, S.G. Lee, S.M. Song, Y.J. Lim, J.H. Lee, S.H. Lee, Fast switchable micro-lenticular lens arrays using highly transparent nano-polymer dispersed liquid crystals, Adv. Mater. Interfaces 6 (18) (2019) 1900841.
[16] N. Noda, J. Obrzut, High frequency dielectric relaxation in polymers filled with ferroelectric ceramics, Materials Research Society Symposium Proceedings, 1999, Materials Research Society, Warrendale, Pa 2002, pp. 113–120.
[17] N.H. Park, S.C. Noh, P. Nayek, M.-H. Lee, M.S. Kim, L.-C. Chien, J.H. Lee, B.K. Kim, S.H. Lee, Optically isotropic liquid crystal mixtures and their application to high-performance liquid crystal devices, Liq. Cryst. 42 (4) (2015) 530–536.
[18] L. Rao, J. Yan, S.-T. Wu, S.-i. Yamamoto, Y. Haseba, A large Kerr constant polymer-stabilized blue phase liquid crystal, Appl. Phys. Lett. 98 (8) (2011), 081109.
[19] R. Manda, S. Pagidi, Y. Heo, Y.J. Lim, M.S. Kim, S.H. Lee, Electrically tunable photonic band gap structure in monodomain blue-phase liquid crystals, NPG Asia Mater. 12 (1) (2020) 1–9.
[20] S. Pagidi, R. Manda, S.S. Bhattacharyya, K.J. Cho, T.H. Kim, Y.J. Lim, S.H. Lee, Superior electro-optics of nano-phase encapsulated liquid crystals utilizing functionalized carbon nanotubes, Compos. Part B 164 (2019) 675–682.
[21] S. Pagidi, R. Manda, Y.J. Lim, S.M. Song, H. Yoo, J.H. Woo, Y.-H. Lin, S.H. Lee, Helical pitch-dependent electro-optics of optically high transparent nano-phase separated liquid crystals, Opt. Express 26 (21) (2018) 27368–27380.
[22] R. Manda, S. Pagidi, M.S. Kim, C.H. Park, H.S. Yoo, K. Sandeep, Y.J. Lim, S.H. Lee, Effect of monomer concentration and functionality on electro-optical properties of polymer-stabilised optically isotropic liquid crystals, Liq. Cryst. 45 (5) (2018) 736–745.
[23] Y.J. Lim, J.H. Yoon, H. Yoo, S.M. Song, R. Manda, S. Pagidi, M.-H. Lee, J.-M. Myoung, S.H. Lee, Fast switchable field-induced optical birefringence in highly transparent polymer-liquid crystal composite, Optic. Mater. Expr. 8 (12) (2018) 3698–3707.
[24] C. Liao, C. Mak, M. Zhang, H.L. Chan, F. Yan, Flexible organic electrochemical transistors for highly selective enzyme biosensors and used for saliva testing, Adv. Mater. 27 (4) (2015) 676–681.
[25] A. Campana, T. Cramer, D.T. Simon, M. Berggren, F. Biscarini, Electrocardiographic recording with conformable organic electrochemical transistor fabricated on resorbable bioscaffold, Adv. Mater. 26 (23) (2014) 3874–3878.
[26] S.-G. Kang, J.-H. Kim, Optically-isotropic nanoencapsulated liquid crystal displays based on Kerr effect, Opt. Express 21 (13) (2013) 15719–15727.
[27] J. Kerr, A new relation between electricity and light: Dielectrified media birefringent, Lond. Edinburgh Dublin Philos. Magaz. J. Sci. 50 (332) (1875) 337–348.
[28] K. Amundson, Electro-optic properties of a polymer-dispersed liquid-crystal film: temperature dependence and phase behavior, Phys. Rev. E 53 (3) (1996) 2412.
[29] Y.J. Lim, Y.E. Choi, J.H. Lee, G.-D. Lee, L. Komitov, S.H. Lee, Effects of three-dimensional polymer networks in vertical alignment liquid crystal display controlled by in-plane field, Opt. Express 22 (9) (2014) 10634–10641.
[30] M. Oh-e, K. Kondo, Response mechanism of nematic liquid crystals using the in-plane switching mode, Appl. Phys. Lett. 69 (5) (1996) 623–625.
[31] A.R. Blythe, T. Blythe, D. Bloor, Electrical Properties of Polymers, Cambridge university press, 2005.
[32] G.P. Montgomery Jr., J.L. West, W. Tamura-Lis, Light scattering from polymer-dispersed liquid crystal films: droplet size effects, J. Appl. Phys. 69 (3) (1991) 1605–1612.